DOI: 10.19884/j.1672-5220.202310004

Adaptive Droop Control for Circulating Current Suppression in Microgrid Based on Fuzzy Logic

WANG Ziping, SHAN Yinghao*
College of Information Science and Technology, Donghua University, Shanghai 201620, China

Abstract: Circulating currents in a microgrid increase the power loss of the microgrid, reduce the operational efficiency, as well as affect the power quality of the microgrid. The existing literature is seldom concerned with methods to suppress the loop currents using fuzzy logic control. In this paper, a method based on fuzzy control of droop coefficients is proposed to suppress the circulating currents inside the microgrid. The method combines fuzzy control with droop control and can achieve the effect of suppressing the circulating currents by adaptively adjusting the droop coefficients to make the power distribution between each subgrid more balanced. To verify the proposed method, simulation is carried out in Matlab/Simulink environment, and the simulation results show that the proposed method is significantly better than the traditional proportional-integral control method. The circulating currents reduce from about 10 A to several nanoamperes, the bus voltage and frequency drops are significantly improved, and the total harmonic distortion rate of the output voltage reduces from 4.66% to 1.06%. In addition, the method used in this paper can be extended to be applied in multiple inverters connected in parallel, and the simulation results show that the method has a good effect on the suppression of circulating currents among multiple inverters.

Key words: circulating current suppression; microgrid; fuzzy logic; droop control
CLC number: TM61 **Document code**: A
Article ID: 1672-5220 (2024) 06-0677-12

Open Science Identity (OSID)

0 Introduction

A microgrid is a small-scale power network composed of various distributed generations (DGs), storage devices, protection devices, etc. The microgrid can operate in two modes: grid-connected and islanded. Typically, it operates in conjunction with the public grid, but it can switch to the islanded mode if it needs to operate independently or if there is an issue with the external grid[1]. In the islanded mode, the microgrid functions as an independent system that ensures its stability. To convert the direct current (DC) power generated by new energy sources into alternating current (AC) power, a microgrid requires multiple inverters connected in parallel. However, because the parameters of each module in the system are not identical, voltage differences between the modules will occur. Even a minor voltage difference can lead to a large circulating current between the modules, affecting the microgrid's stability due to the small line impedance[2].

The definition and characteristics of circulating currents in parallel inverter systems have been extensively studied. Two types of circulating currents in two inverter systems were defined and then extended to circulating currents in multiple inverter systems[3]. The circulating current suppression method of the DC microgrid operating in the islanded mode was provided with a secondary leakage integral controller based on adaptive linear impedance[4]. A circulating current suppression method between parallel battery energy storage systems in the DC microgrid was proposed, involving the estimation of line impedance through mathematical calculation[5]. The concept of an equivalent feeder to compensate for the difference in feeder impedance was developed, where a control method combining improved droop control and adaptive virtual impedance control was involved[6].

Wei et al.[7] proposed a method for suppressing circulating currents based on a distributed control method that adjusts the original current reference for three-phase voltage source inverters (VSIs). An adaptive virtual impedance control method for distributed generation units in the microgrid to compensate for the circulating currents caused by mismatched branch impedance was designed[8]. A repetitive control method was developed to reduce the harmonic circulating currents between modules in the modular multilevel converter[9]. A control method for modular multilevel converter-high voltage DC under unbalanced grid conditions was studied, in which the proportional resonant (PR) controller was used to

Received date: 2023-10-14
Foundation items: National Natural Science Foundation of China (No. 62303107); Fundamental Research Funds for the Central Universities, China (Nos. 2232022G-09 and 2232021D-38); Shanghai Sailing Program, China (No. 21YF1400100)
* Correspondence should be addressed to SHAN Yinghao, email: shanyh@dhu.edu.cn
Citation: WANG Z P, SHAN Y H. Adaptive droop control for circulating current suppression in microgrid based on fuzzy logic[J]. *Journal of Donghua University (English Edition)*, 2024, 41(6): 677-688.

suppress circulating currents[10].

In recent years, fuzzy control has gained popularity as an effective method for microgrid control[11]. As opposed to traditional control methods which rely on a specific mathematical model of the controlled object, fuzzy control simulates the thinking and the judgment of the human brain through computer simulation[12]. This allows the system to achieve control without the need for a specific mathematical model and can overcome the influence of nonlinear factors in the system[13]. By leveraging the power of fuzzy logic, fuzzy control can achieve more robust and reliable control of microgrid systems. Additionally, fuzzy control can be easily adapted to different types of microgrid systems, making it a versatile option for a wide range of applications.

Fuzzy control is used for the energy management system of an intelligent microgrid in a residential area[14]. It designs two types of fuzzy control, where the membership functions define the power transmission amount and direction from and to the main grid. A virtual synchronous generator (VSG) control method based on a fuzzy logic controller (FLC) was proposed to adjust the governor's power by changing the voltage phase angle and frequency to increase inertia[15]. A fuzzy quadratic controller-based VSG control scheme was presented to improve voltage and frequency regulation, as well as the dynamic performance of the microgrid[16]. A multitask fuzzy control that only acted on quadratic control was proposed to allow for frequency and voltage regulation in both islanded and grid-connected modes[17]. A fuzzy control method for distributed generation units and their loads operating in the islanded mode was presented[18], where black-box nonlinear optimization techniques were utilized to adjust the membership functions. Fuzzy control was used for the energy management system of a residential microgrid operating in grid-connected mode to minimize grid power fluctuations[19]. A fuzzy control scheme for the microgrid and distributed energy sources was proposed to use a nonlinear FLC to control the reactive power reference, and the robustness of the system was improved[20]. An enhanced fuzzy control method was proposed to stabilize the microgrid by reducing the circulating currents between the DC loop and the energy storage system[21].

To sum up, there is already a considerable amount of literature on separately investigating circulating current suppression and fuzzy control in the microgrid. However, research regarding the utilization of fuzzy control to achieve circulating current suppression in the microgrid is still inadequate, particularly through the alteration of droop control coefficients. In this paper, according to the droop control, the difference in power distribution between two inverters can be reduced by changing the droop coefficients; fuzzy control can adaptively adjust the droop coefficients, which in turn reduces the circulating currents in the system, and the power difference between the two inverters will become smaller and smaller to realize the equal distribution of active and reactive power. Thus, this paper aims to conduct comprehensive research on this subject. The microgrid configuration studied herein is depicted in Fig. 1.

Figure 1 illustrates two DGs that are connected via an AC bus to supply local and common loads. The main circuitry of the DG is powered by a photovoltaic (PV) DC source and includes a three-phase full-bridge inverter with a passive filter (L_f, C_f, L). The system control loop is split into two main parts: power sharing and voltage & current dual loop. In the power sharing part, the inverter output's active power P and reactive power Q are determined by sampling the three-phase voltage U_{0a}, U_{0b} and U_{0c}, and current I_{0a}, I_{0b} and I_{0c} at the inverter output side. I_1 is the output current. In addition, f_n, U_n, P_n and Q_n in this part are the reference values for frequency, voltage, active power and reactive power, respectively. These values are then substituted into the active power-frequency (P-f) and reactive power-terminal voltage (Q-U) droop equations to obtain the frequency and output voltage amplitude references of the inverter. The voltage & current dual loop is then used to adjust the inverter output voltage using pulse width modulation (PWM).

This paper makes the following main contributions. 1) Fuzzy control is used to adaptively adjust droop coefficients, which leads to the suppression of circulating currents. 2) Power allocation is proportionally distributed while suppressing circulating currents, and the waveform quality is significantly improved.

The organization structure of the remaining part of this paper is as follows: Section 1 introduces the inverter control of the microgrid; Section 2 designs an FLC and introduces it to the circulating current suppression; Section 3 conducts simulation analysis and result discussion; Section 4 provides the conclusion.

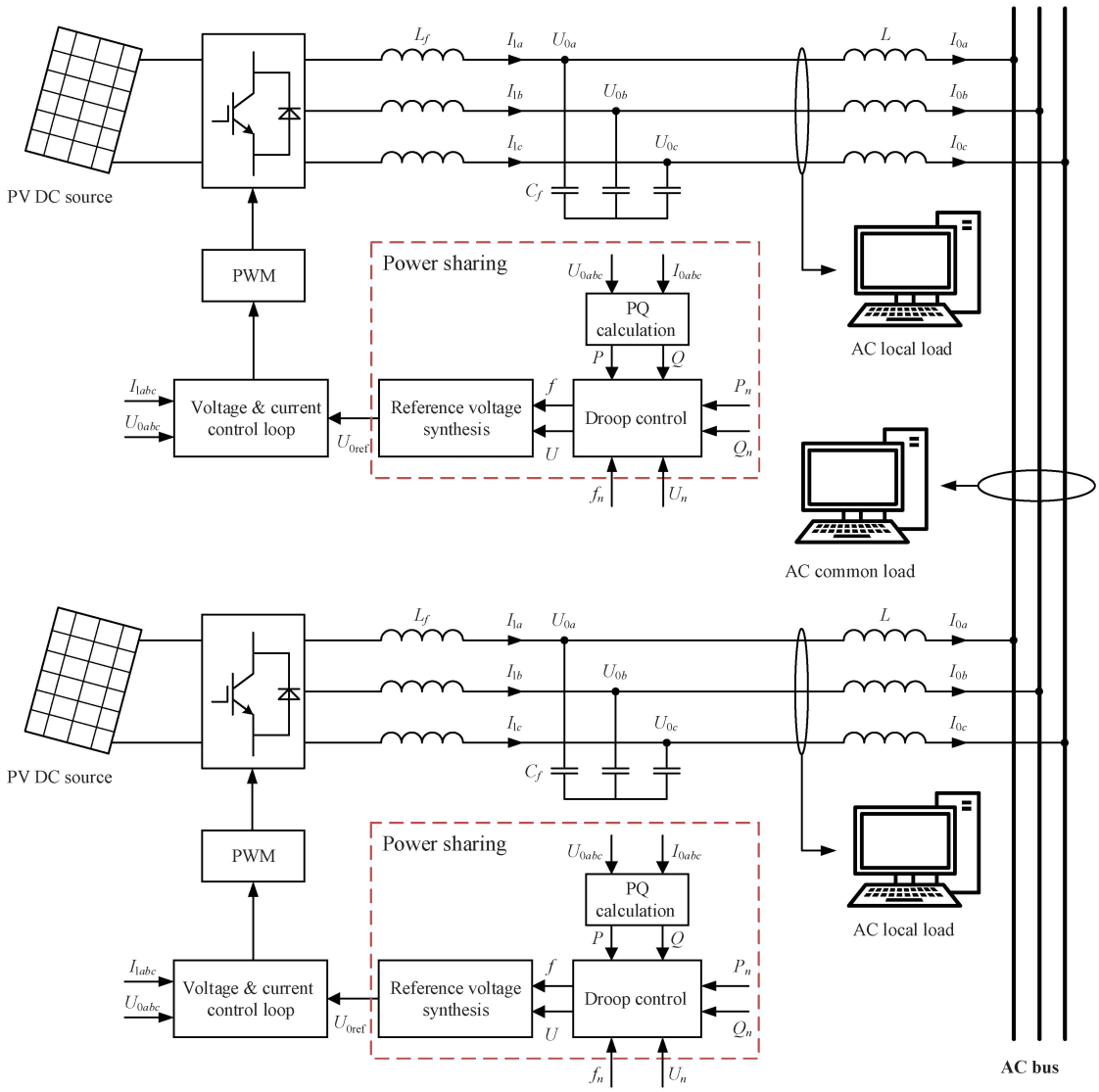

Fig. 1 Configuration of microgrid

1 Inverter Control of Microgrid

1.1 Droop control

Droop control is widely used due to its advantages of no interconnection and plug-and-play. It simulates the droop characteristics of synchronous generators in traditional power systems to control inverters, resulting in stable frequency and voltage. *P-f* droop and *Q-U* droop characteristics are shown in Fig. 2. When the microgrid is in steady state operation, the two operating points of the inverter (f_0, P_0, U_0, Q_0) and (f_1, P_1, U_1, Q_1) are taken. To understand the principle of droop control and power transmission, a simplified parallel equivalent circuit that incorporates two inverters is utilized as shown in Fig. 3.

In Fig. 3, $U_1\angle\varphi_1$ and $U_2\angle\varphi_2$ are the no-load output voltage of inverters 1 and 2, respectively; φ_1 and φ_2 are the no-load output voltage phases of inverters 1 and 2, respectively; $E\angle 0$ is the parallel bus voltage; $Z_i\angle\theta_i = R_i + jX_i$ is the sum of the output impedance and line impedance of the inverter, with $i = 1, 2$; θ_i is the impedance angle, which is equal to $\theta_i = \arctan(R_i/X_i)$; Z_L is the common load impedance; I_0 is the common bus current; I_{L1} and I_{L2} are the output currents of inverters 1 and 2, respectively.

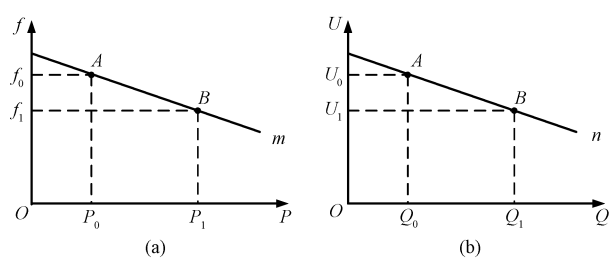

Fig. 2 Curves of droop control characteristics: (a) *P-f*; (b) *Q-U*

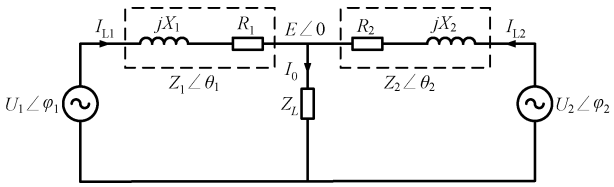

Fig. 3 Diagram of parallel equivalent circuit with two inverters

The inverter's active power P and reactive power Q can be obtained as

$$P_i = \frac{1}{|Z_i|}[(EU_i\cos\varphi_i - E^2)\cos\theta_i + EU_i\sin\varphi_i\sin\theta_i], \quad (1)$$

$$Q_i = \frac{1}{|Z_i|}[(EU_i\cos\varphi_i - E^2)\sin\theta_i - EU_i\sin\varphi_i\cos\theta_i], \quad (2)$$

where $|Z_i|$ is the impedance magnitude corresponding to the ith inverter; E is the voltage amplitude of the inverter; φ_i is the phase angle of the no-load output voltage of the ith inverter.

$$|Z_i| = \sqrt{R_i^2 + X_i^2}. \quad (3)$$

When $Z_i\angle\theta_i$ is inductive, the droop control formula can be derived as

$$\begin{cases}\omega_i = \omega_i^* - mP_i,\\ U_i = U_i^* - nQ_i,\end{cases} \quad (4)$$

where ω_i^* and U_i^* are the frequency and amplitude of the unloaded output voltage, respectively; m and n are the corresponding droop coefficients, respectively.

As P and Q of the DG increase, the operating point moves from point A to point B (Fig. 2). For small phase angles δ (or power angles) between the inverter and the grid, the droop control gives the following relationship:

$$\begin{cases}f = f_n - m(P - P_n),\\ U = U_n - n(Q - Q_n),\end{cases} \quad (5)$$

In the power control module, the instantaneous power output of the inverter is

$$\begin{cases}P = u_d i_d + u_q i_q,\\ Q = u_q i_d - u_d i_q,\end{cases} \quad (6)$$

where u_d and u_q are the instantaneous inverter voltages on the grid side, respectively; i_d and i_q are the instantaneous inverter output currents, respectively.

1.2 Model of VSIs and coordinate transformation

There are two types of three-phase inverters: voltage source and current source. VSIs are more commonly used due to their faster current regulation and ability to react quickly to changes. VSIs use a three-phase full-bridge topology with an LC filter to produce the three-phase output voltage. Converting three-phase abc coordinates into dq rotating coordinates simplifies controller design and control algorithms, allowing for easy separation of DC and AC components. According to the Clarke transform, converting three-phase abc coordinates into components that reside in the stationary $\alpha\beta$ coordinate system. Next, according to the Park transforms, the $\alpha\beta$ stationary coordinate components are transformed into components in the dq rotational coordinate system, and the purpose of multiplying by 2/3 is to keep the amplitude of the currents before and after the transformation constant.

$$\boldsymbol{T}_{abc-\alpha\beta} = \frac{2}{3}\begin{bmatrix}1 & -\frac{1}{2} & -\frac{1}{2}\\ 0 & \frac{\sqrt{3}}{2} & -\frac{\sqrt{3}}{2}\end{bmatrix}, \quad (7)$$

$$\boldsymbol{T}_{\alpha\beta-dq} = \begin{bmatrix}\cos(\omega t) & \sin(\omega t)\\ -\sin(\omega t) & \cos(\omega t)\end{bmatrix}, \quad (8)$$

where ω is the angular frequency; t is the time.

1.3 Voltage and current dual closed-loop control system

To synchronize voltage and frequency between the microgrid and the main power grid, a dual closed-loop control system was used. The reference voltage amplitude was compared with the inverter's real-time output voltage by the voltage outer loop control, which used propotional-integral (PI) control to stabilize the load voltage. The current inner loop control system used PI control to improve the system response speed and PWM to control the inverter. The dual closed-loop control diagram is shown in Fig. 4. In Fig. 4, U_{refd} and U_{refq} are reference voltages on the d axis and q axis after voltage synthesis, respectively; U_{0d} and U_{0q} are the bus voltage on the d axis and q axis, respectively; I_{0d} and I_{0q} are the corresponding current flows.

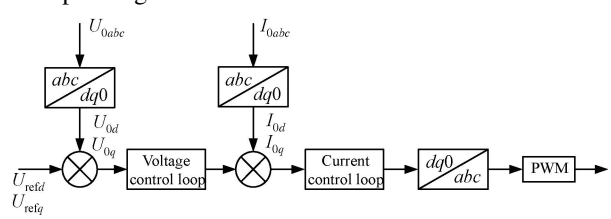

Fig. 4 Dual closed-loop control diagram

The components of voltage and current on the dq axis are obtained by performing the Park transformation of AC voltage and current. The Park transformation equation is

$$\begin{cases}X_d = \sqrt{\frac{2}{3}}\left[X_a\sin(\omega t) + X_b\sin\left(\omega t - \frac{2\pi}{3}\right) + X_c\sin\left(\omega t + \frac{2\pi}{3}\right)\right],\\ X_q = \sqrt{\frac{2}{3}}\left[-X_a\cos(\omega t) - X_b\sin\left(\omega t - \frac{2\pi}{3}\right) - X_c\sin\left(\omega t + \frac{2\pi}{3}\right)\right].\end{cases} \quad (9)$$

2 Design of FLC and Application in Circulating Current Suppression

2.1 Fuzzy variables and membership functions

Figure 5 depicts the control flow diagram of the FLC, with the following basic control rules.

1) Select input & output fuzzy set: convert inputs to fuzzy variables.

2) Define input & output membership function: determine fuzzy linguistic values and select membership functions. Variables are scaled according to membership functions.

3) Design fuzzy rule: based on experience, a fuzzy rule base is established, containing control relationships for fuzzy variables.

4) Establish fuzzy control form: implements decision-making based on membership functions and rule base.

5) Fuzzy reasoning: process control quantity obtained from inference in reverse and convert it to a control output.

6) Unite fuzzy: applying the fuzzy output values obtained from the fuzzy control system to the real controlled model.

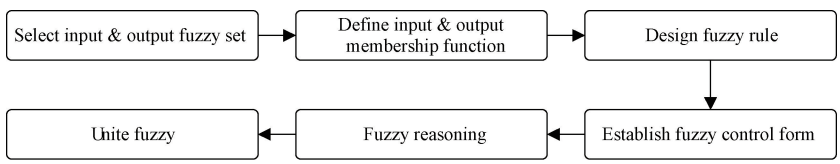

Fig. 5 Control flow diagram of FLC

Fuzzy control is a smart and nonlinear control method that mimics human thinking to control the system without the need for a specific mathematical model of the object. The rule base is important and affects the control effectiveness. A detailed rule base reduces steady-state errors but increases complexity, while a smaller rule base increases steady-state errors but simplifies the calculation. Fuzzy process has three steps: fuzzification, fuzzy inference and defuzzification.

In the microgrid, four values (u_d, u_q, i_d and i_q) are obtained by transforming three-phase voltages. These data are then input into an FLC which fuzzifies the input and performs inference based on a knowledge base. The inference process depends on the controller's design rules and membership functions. The output is obtained by defuzzifying the output fuzzy variables. To adaptively adjust the *P-f* and *Q-U* droop coefficients in one DG, two FLCs are needed based on the designed microgrid model. Figure 6 displays the membership functions for both controllers.

In Fig. 6, the same membership functions are used for the inputs and outputs of the two controllers in this study. The basic domain of the inputs and outputs is $[-6, 6]$, and the basic domain of the fuzzy control input and output variables are quantized within the fuzzy sets $\{-6, -4, -2, 0, 2, 4, 6\}$. The corresponding linguistic variable sets are {negative big (NB), negative medium (NM), negative small (NS), zero (0), positive small (PS), positive medium (PM), positive big (PB)}.

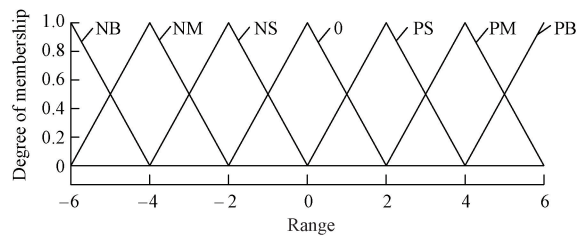

Fig. 6 Fuzzy variables and their membership functions

2.2 Fuzzy inference and defuzzification

Fuzzy rules rely on binary fuzzy relationships. The rule follows the format "if x is A, then y is B", with A representing the premise of the fuzzy rule and B representing the conclusion derived through fuzzy inference. A and B can be NB, NM, NS, 0, PS, PM and PB. The effectiveness of fuzzy control is directly influenced by the rule base. Table 1 displays the fuzzy rule base created using the expertise of engineers and technicians with control experience.

Table 1 Fuzzy rule

m_p/m_q		e_p, e_q						
		NB	NM	NS	0	PS	PM	PB
Δe_p, Δe_q	NB	PB/NB	PB/NB	PB/NM	PB/NM	PM/NS	0/0	0/0
	NM	PB/NB	PB/NB	PB/NM	PB/NS	PM/NS	0/0	0/0
	NS	PM/NB	PM/NM	PM/NS	PM/NS	0/0	NS/PS	NS/PS
	0	PM/NM	PM/NM	PS/NS	0/0	NS/PS	NM/PM	NM/PM
	PS	PS/NM	PS/NS	0/0	NM/PS	NM/PS	NM/PM	NM/PB
	PM	0/0	0/0	NM/PS	NB/PS	NB/PM	NB/PB	NB/PB
	PB	0/0	0/0	NM/PS	NB/PM	NB/PM	NB/PB	NB/PB

To interpret Table 1, e_p and e_q represent the error between the actual output and the expected output, respectively; Δe_p and Δe_q represent the error rate between the actual output and the expected output, respectively; m_p and m_q represent the degree of membership. For instance, if e_p and e_q are NB and Δe_p and Δe_q are also NB, then m_p takes PB, and m_q takes NB. Other cases follow similar rules. In total, there are 49 rules. The selection of rules is based on finding a balance between the complexity of the FLC and the estimated error. The inference mechanism uses Mamdani's max-min method and defuzzification utilizes the center of the gravity method to produce m_p and m_q, as described in this paper. The output obtained through fuzzy inference needs to be defuzzified. There are many methods for defuzzification, including the centroid method, the weighted average method and the maximum membership degree method. The method of defuzzy requires that the results of the operation of the output affiliation function can be well calculated. The centroid method is to find the gravity center of the area enclosed by the horizontal coordinate axis and the curve of the affiliation function and use this center of gravity as the output value of the fuzzy inference. The centroid method has a smoother output operation. Even if it corresponds to a small change in the input signal, the output will change accordingly. The corresponding fuzzy logic rule surface plot is provided in Fig. 7.

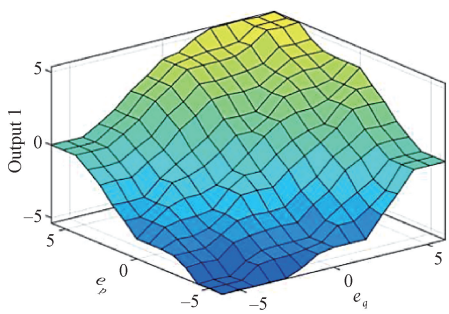

Fig. 7 Fuzzy logic rule surface plot

2.3 Microgrid circulating current characteristics

The parallel operation of multiple DGs can realize large-capacity and redundant power supply of the microgrid, improve the flexibility and reliability of system power supply, and have a broad application prospect. To ensure a stable microgrid and interconnected system operation, it's important to control the circulating current between inverters. Traditional droop control can result in different output voltages of inverters due to differences in hardware, software, line impedance, filtering parameters and DC source output voltage. Therefore, traditional droop control always causes circulating currents between inverters, decreases transmission efficiency, destabilizes the system, and compromises its safety. Next, an equivalent schematic is used to analyze the system's circulating currents, which includes two or more parallel DGs. Figure 8 shows the equivalent schematic of two parallel inverters.

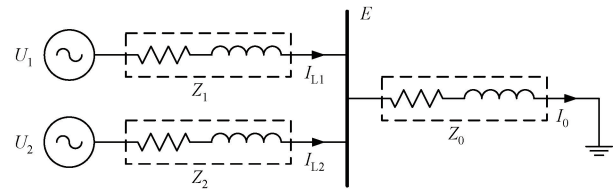

Fig. 8 Equivalent schematic of two parallel inverters

In Fig. 8, when local loads are not considered, let I_{L1} and I_{L2} be the output currents of inverters 1 and 2, respectively:

$$I_{L1}=\frac{U_1-E}{Z_1},\ I_{L2}=\frac{U_2-E}{Z_2}. \tag{10}$$

According to Millman's theorem, we can get:

$$E=\frac{(U_1/Z_1)+(U_2/Z_2)}{(1/Z_1)+(1/Z_2)+(1/Z_0)}=\frac{Z_0(U_1Z_2+U_2Z_1)}{Z_1Z_2+Z_2Z_0+Z_1Z_0}. \tag{11}$$

The circulating current I_H is defined as

$$I_H=\frac{1}{2}(I_{Li}-I_{Lk}),\ (i,k=1,2;\ i\neq k). \tag{12}$$

Then the circulating currents between inverters 1 and 2 are expressed by

$$\begin{cases} I_{H1}=\dfrac{1}{2}(I_{L1}-I_{L2}), \\ I_{H2}=\dfrac{1}{2}(I_{L2}-I_{L1}). \end{cases} \tag{13}$$

It can be seen that the magnitude of the circulating currents between inverters 1 and 2 is equal, but the direction is opposite.

$$I_0=I_{L1}+I_{L2}. \tag{14}$$

By combining Eqs. (13) and (14), we get:

$$\begin{cases} I_{H1}=I_{L1}-\dfrac{1}{2}I_0, \\ I_{H2}=I_{L2}-\dfrac{1}{2}I_0. \end{cases} \tag{15}$$

After rearrangement, circulating currents between the two inverters are expressed by

$$\begin{cases} I_{H1}=\dfrac{Z_2(U_1-E)-Z_1(U_2-E)}{2Z_1Z_2}, \\ I_{H2}=\dfrac{Z_1(U_2-E)-Z_2(U_1-E)}{2Z_1Z_2}. \end{cases} \tag{16}$$

From the above equations, it can be seen that the magnitude of the circulating currents is related to the output voltage of the inverter and the line impedance. When the output voltage amplitude and phase of the two inverters are the same and the line impedance is

consistent, the circulating current is zero.

Figure 9 shows the equivalent schematic diagram of n parallel inverters. The output current of the kth ($k=1, 2, \cdots, n$) inverter I_{Lk} is given by

$$I_{Lk} = \frac{U_k - E}{Z_k}. \tag{17}$$

Again, according to Millman's theorem, we can get:

$$E = \frac{\dfrac{U_1}{Z_1} + \dfrac{U_2}{Z_2} + \cdots + \dfrac{U_n}{Z_n}}{\dfrac{1}{Z_1} + \dfrac{1}{Z_2} + \cdots + \dfrac{1}{Z_n} + \dfrac{1}{Z_0}} = \frac{\sum_{i=1}^{n} \dfrac{U_i}{Z_i}}{\sum_{i=0}^{n} \dfrac{1}{Z_i}}. \tag{18}$$

The total circulating current of inverter k I_{Hk} is given by

$$I_{Hk} = I_{Lk} - \frac{1}{n} I_0, \tag{19}$$

where $I_0 = I_{L1} + I_{L2} + \cdots + I_{Ln}$.

By combining Eqs. (18) and (19), we get:

$$I_{Hk} = \frac{n(U_k - E)\prod_{\substack{i=1 \\ i\neq k}}^{n} Z_i - \sum_{i=1}^{n}\left[(U_i - E)\prod_{\substack{j=1 \\ j\neq i}}^{n} Z_j\right]}{n\prod_{i=1}^{n} Z_i}. \tag{20}$$

This is the expression of the circulating current for the kth inverter.

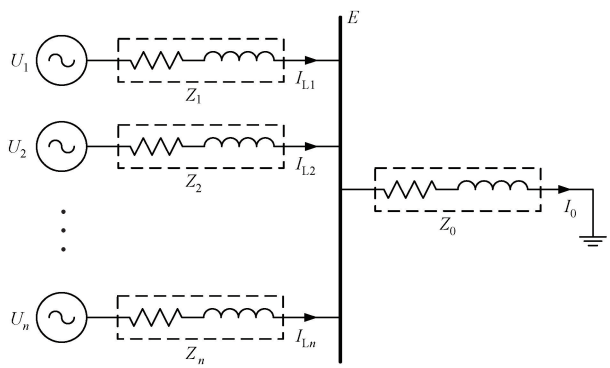

Fig. 9 Equivalent schematic diagram of n parallel inverters

2.4 Circulating current suppression using fuzzy control

The input signals of the FLC are P and Q outputs by the inverter. Based on the structure of droop control, the following formula can be obtained:

$$\begin{cases} f = f_n - \alpha_1(P - P_n)\beta_1[fuzzy], \\ U = U_n - \alpha_2(Q - Q_n)\beta_2[fuzzy]. \end{cases} \tag{21}$$

The output of the FLC consists of f and U which are subtracted from the grid frequency f_n and the voltage U_n, respectively. The gains of the input and output signals of the FLC are denoted by α_1, α_2, β_1 and β_2. The active and reactive powers are subtracted from their respective references to generate input signals e_p and e_q. Their rates of change are represented by Δe_p and Δe_q, respectively. The fuzzy control diagram is shown in Fig. 10.

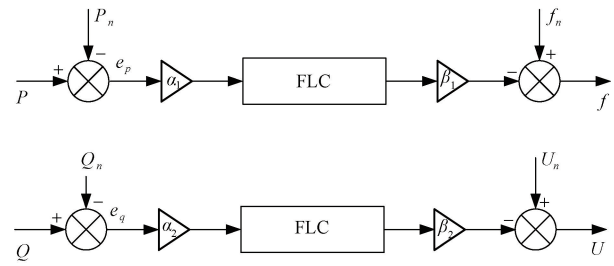

Fig. 10 Fuzzy control diagram

3 Simulation and Analysis of Microgrid and Circulating Current Suppression

To test the practicality and the efficiency of the adaptive adjustment method for the droop coefficient in fuzzy control, and its potential use in circulating current suppression, we established and analyzed a microgrid model using the MATLAB/Simulink simulation platform. The microgrid's operating parameters are listed in Table 2.

Table 2 System setting and control parameter

Parameter		Value
Source voltage/kV		1
AC filter	C/μF	250
	L/mH	0.9
Droop coefficient		$m_1 = 3/70\,000$, $n_1 = 4/110\,000$; $m_2 = 3/80\,000$, $n_2 = 1/3\,000$
Fuzzy gain coefficient		$\alpha_1 = 0.1$, $\alpha_2 = 0.1$; $\beta_1 = 10$, $\beta_2 = 10$

Assuming that the microgrid is initially operating in islanded mode, load 3 (20 kW) is connected to the microgrid at $t=1$ s, and then disconnected at $t=2$ s. This allows us to observe the circulating current variation of the microgrid during this period.

3.1 Circulating current characteristics of microgrid based on fuzzy control

PI control is widely used with the droop control of the inverter, and the selection of its parameters directly affects the control effect of the inverter. The parameter setting of PI control is more complicated, and the fixed parameters are less flexible and adaptable in response to changes in external operating conditions with greater limitations. However, fuzzy control avoids this, and the parameters can be adjusted in real-time, with good dynamic performance. In Fig. 11(a), the black line shows the circulating currents between the two inverters when only PI control is implemented with $P=2$ and $I=50$. The red line represents the circulating currents between the two inverters when applying fuzzy control at

the droop coefficient.

Figure 11 (b) presents a magnified view of the circulating current achieved with fuzzy control. The image clearly shows that the circulating current is nearly zero, indicating a successful suppressing effect. The peak value of the circulating current has been effectively reduced from 8 A to almost zero, demonstrating that fuzzy control significantly suppresses the circulating current.

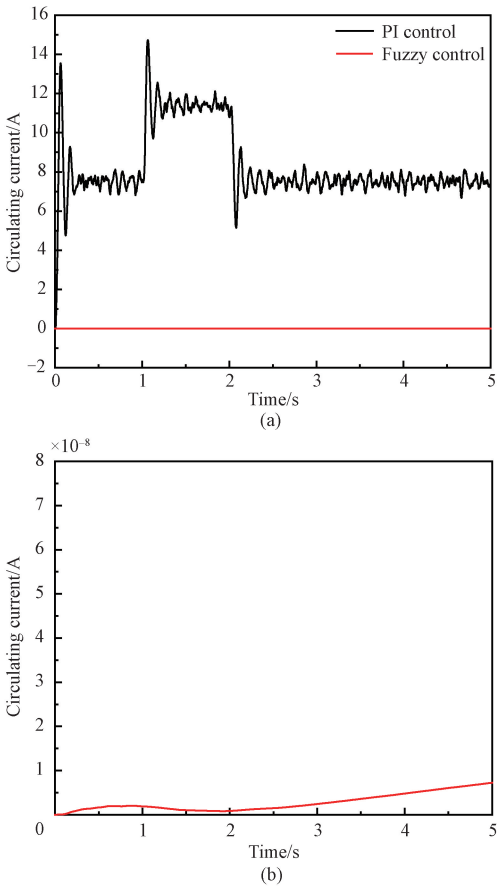

Fig. 11 Circulating current: (a) PI control and fuzzy control; (b) magnified view of fuzzy control

Changes in the active and reactive powers are observed as the load varies. During the islanded mode, load 3 is connected to the microgrid at $t = 1$ s and then disconnected at $t = 2$ s. The simulation results of the two inverters DG1 and DG2 are shown in Figs. 12 and 13.

According to the droop control characteristics, when load 3 is connected to the microgrid from the period of 1 s to 2 s, this results in the drop of the terminal voltage and frequency, as shown in Figs. 14 and 15.

When traditional droop control is used, the active and reactive powers cannot be evenly distributed, and the circulating current is mainly caused by the uneven distribution of powers. As the increase of load, the circulating current also increases accordingly.

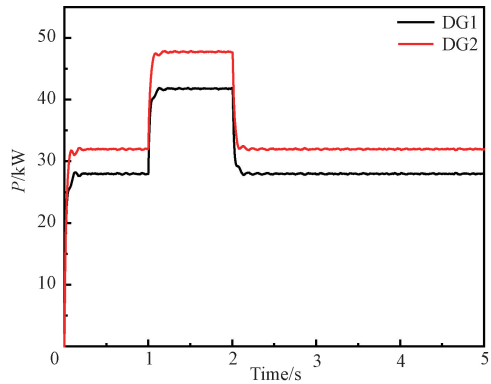

Fig. 12 Active power sharing of PI control

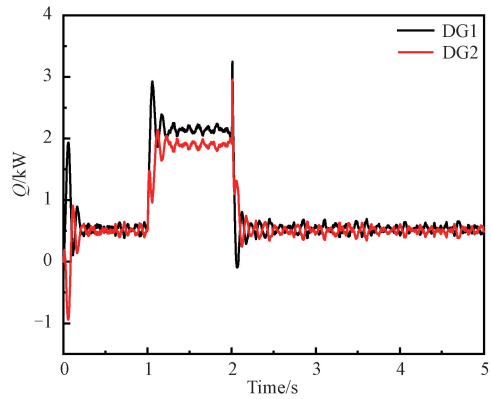

Fig. 13 Reactive power sharing of PI control

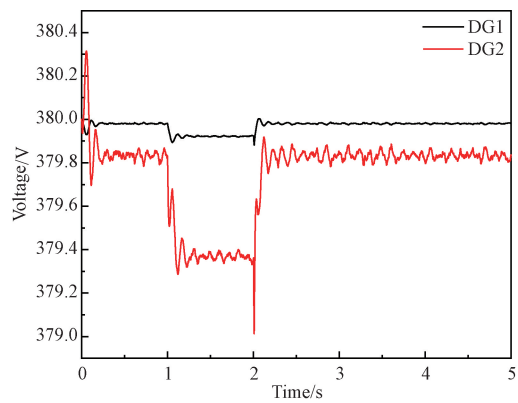

Fig. 14 Bus voltage amplitude of PI control

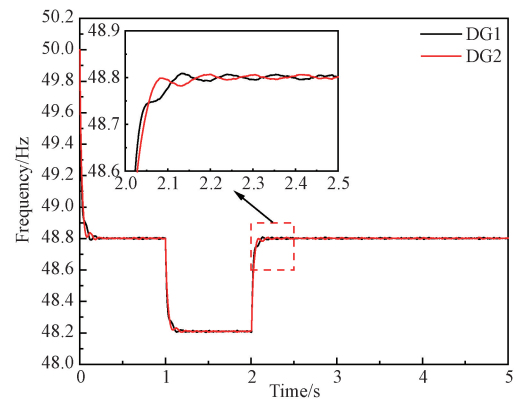

Fig. 15 System frequency of PI control

The fast Fourier transform (FFT) is used to calculate the total harmonic distortion (THD) of the output voltage U, resulting in 4.66%, as shown in Fig. 16. It is clear that the main harmonic in the inverter and system is the 2nd harmonic.

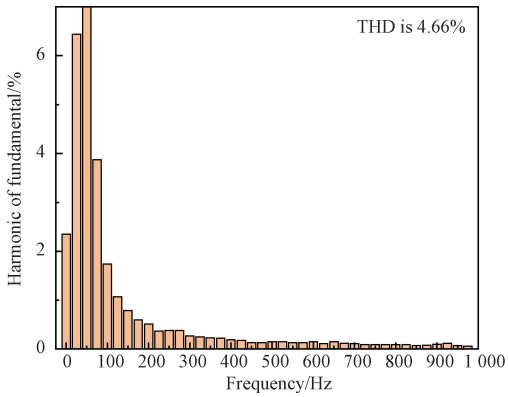

Fig. 16 FFT analysis of PI control

3.2 Circulating current characteristics of microgrid based on fuzzy control droop coefficient

Fuzzy control is utilized to adaptively adjust the droop coefficient, reducing the difference in power distribution between two inverters and thereby reducing circulating currents. This leads to a reduction in the power difference between the two inverters DG1 and DG2, thereby achieving an equal distribution of active power and reactive power. After implementing fuzzy control, the active power and reactive power outputs of DG1 and DG2 are shown in Figs. 17 and 18, respectively. It can be seen that after the fuzzy control adjustment, the power outputs of the two inverters DG1 and DG2 are more balanced, the power difference is reduced, and the circulating current problem is effectively mitigated.

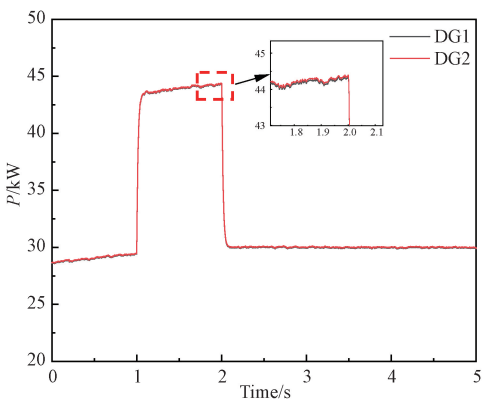

Fig. 17 Active power sharing of fuzzy control

The use of fuzzy control significantly reduces the voltage and the frequency drop amplitude. The bus voltage amplitude and system frequency are shown in Figs. 19 and 20, respectively. It can be seen that after the application of fuzzy control, the fluctuation amplitude of the voltage and frequency of DG1 and DG2 is significantly reduced, and the stability of the system is significantly improved.

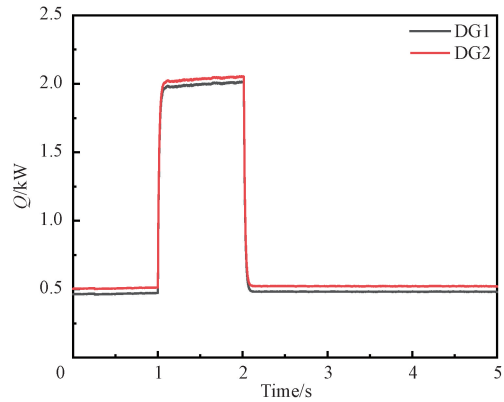

Fig. 18 Reactive power sharing of fuzzy control

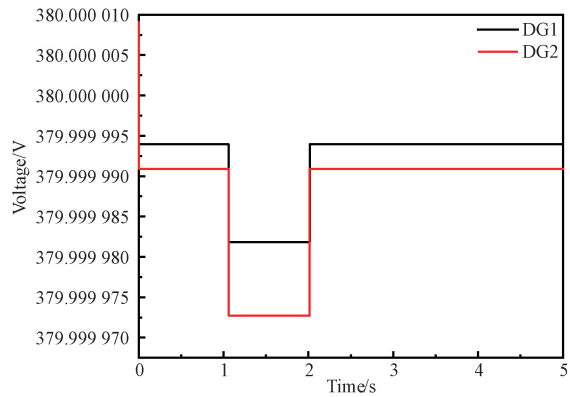

Fig. 19 Bus voltage amplitude with fuzzy control

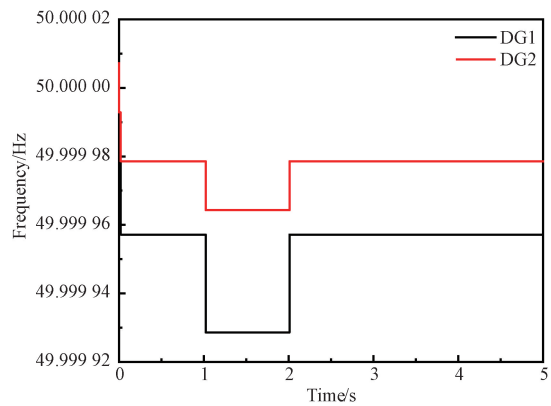

Fig. 20 System frequency with fuzzy control

The simulation results show that fuzzy control effectively improves the power distribution in the system. Under the condition that the control parameters of both inverters are completely identical, the power is reasonably evenly distributed. The THD value is recalculated in this section by performing an FFT transformation on the output voltage U. The recalculated THD value is 1.06%, as shown in Fig. 21.

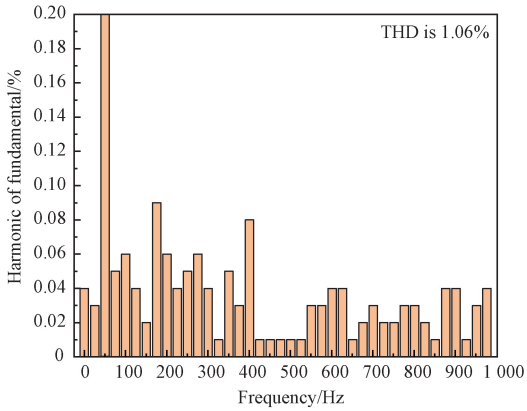

Fig. 21 FFT analysis of fuzzy control

Figure 21 displays an FFT analysis with fuzzy control. The main harmonics in the inverter and the system are identified as the 4th and 8th harmonics. Under previous droop control, the THD of the output voltage reached 4.66%, while after incorporating fuzzy control, the THD of the output voltage was reduced to 1.06%. Both THD values are less than 5%, but the THD after adding fuzzy control is significantly lower, indicating an improved output voltage waveform.

3.3 Circulating current characteristics of n ($n>2$) inverters in parallel

Based on the generalization from two inverters in parallel, applying PI control and fuzzy control to n ($n>2$) inverters in parallel and the circulating current of each inverter is observed. Figure 22 shows the circulating currents between each inverter controlled by PI when $n=3$. Figure 23 displays the circulating currents between each inverter when fuzzy control is applied to the droop coefficient.

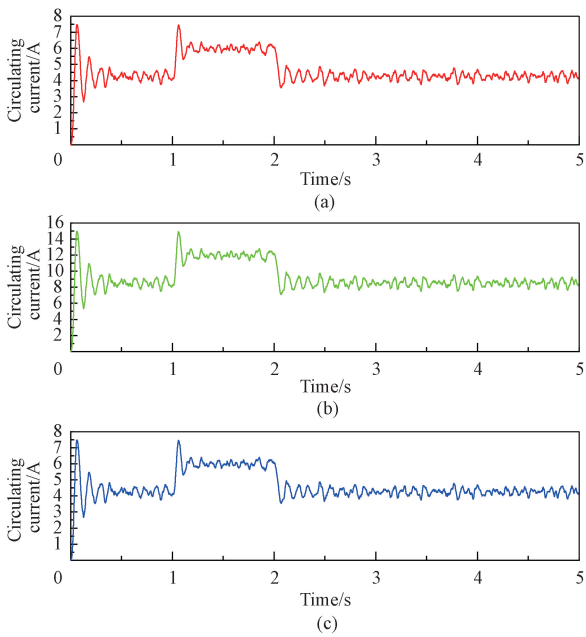

Fig. 22 Circulating currents of three inverters controlled by PI: (a) inverter 1; (b) inverter 2; (c) inverter 3

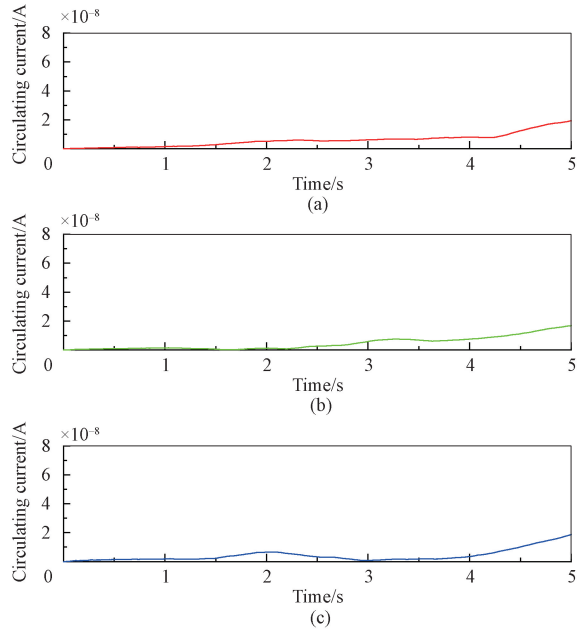

Fig. 23 Circulating currents of three inverters controlled by fuzzy: (a) inverter 1; (b) inverter 2; (c) inverter 3

Then, paralleling $n=3$ inverters is further explored, and $n=4$ is analyzed to investigate the circulating current in the system. When $n=4$, the circulating currents between each inverter controlled by PI are shown in Fig. 24. Figure 25 shows the circulating currents between each inverter when the droop coefficient is subjected to fuzzy control. By using the proposed fuzzy control method, it has been proven that circulating currents can be effectively reduced when several inverters (three, four, or more) are linked in parallel.

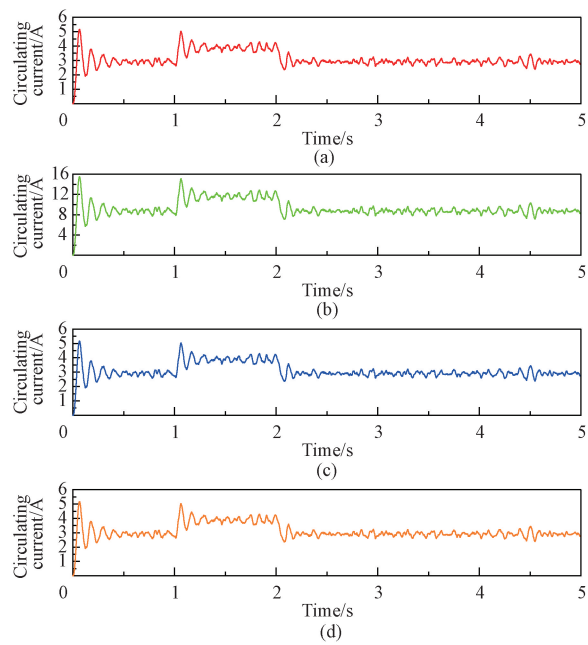

Fig. 24 Circulating currents of four inverters controlled by PI: (a) inverter 1; (b) inverter 2; (c) inverter 3; (d) inverter 4

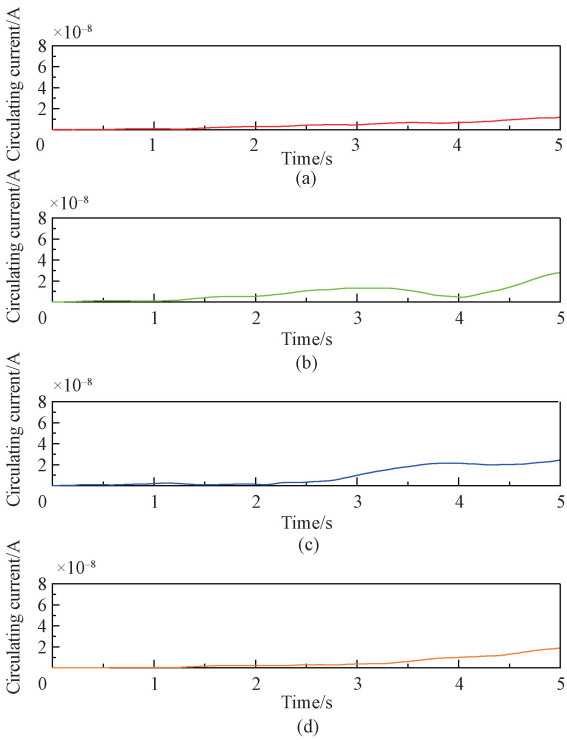

Fig. 25 Circulating currents of four inverters controlled by fuzzy: (a) inventer 1; (b) inventer 2; (c) inventer 3; (d) inventer 4

4 Conclusions

This paper presented a method to suppress circulating currents in a microgrid using fuzzy control. The droop control in the microgrid was adaptively adjusted by applying fuzzy control to the droop coefficient through 49 defined rules based on engineer experience. MATLAB/Simulink was used to develop the microgrid model and to compare the circulating currents under two conditions: with conventional PI control and with the proposed fuzzy control applied to the droop coefficient. Results showed that the proposed method effectively reduced circulating currents between inverters, evenly distributed the active and reactive power outputs of the microgrid, and significantly decreased the THD of the output voltage, resulting in improved voltage quality. It is also advisable to use the proposed fuzzy control to effectively decrease circulating currents when multiple inverters are connected in parallel.

References

[1] CHE L, SHAHIDEHPOUR M, ALABDULWAHAB A, et al. Hierarchical coordination of a community microgrid with AC and DC microgrids [J]. *IEEE Transactions on Smart Grid*, 2015, 6(6): 3042-3051.

[2] ZHANG C H, LI X Y, XING X Y, et al. Modeling and mitigation of resonance current for modified LCL-type parallel inverters with inverter-side current control [J]. *IEEE Transactions on Industrial Informatics*, 2022, 18(2): 932-942.

[3] ROSLAN M A, AHMAD M S, ISA M A M, et al. Circulating current in parallel connected inverter system [C]//2016 IEEE International Conference on Power and Energy (PECon). Melaka: IEEE, 2016: 172-177.

[4] ODO P. Suppression of circulating current in islanded DC microgrid using a decentralized adaptive line resistance approach with secondary leaky integration control [C]//2022 4th Global Power, Energy and Communication Conference (GPECOM). New York: IEEE, 2022: 32-36.

[5] SHAN Y H, HU J F, CHAN K W, et al. Model predictive control of bidirectional DC-DC converters and AC/DC interlinking converters: a new control method for PV-wind-battery microgrids [J]. *IEEE Transactions on Sustainable Energy*, 2019, 10(4): 1823-1833.

[6] ZHANG M R, SONG B H, WANG J Y. Circulating current control strategy based on equivalent feeder for parallel inverters in islanded microgrid [J]. *IEEE Transactions on Power Systems*, 2019, 34(1): 595-605.

[7] WEI B Z, GUERRERO J M, VÁSQUEZ J C, et al. A circulating-current suppression method for parallel-connected voltage-source inverters with common DC and AC buses [J]. *IEEE Transactions on Industry Applications*, 2017, 53(4): 3758-3769.

[8] PHAM M D, LEE H H. Adaptive virtual impedance control method for accurate reactive power sharing and circulating current suppression in islanded microgrid [C]//2019 IEEE Student Conference on Electric Machines and Systems (SCEMS 2019). New York: IEEE, 2019: 1-5.

[9] HE L Q, ZHANG K, XIONG J, et al. A repetitive control scheme for harmonic suppression of circulating current in modular multilevel converters [J]. *IEEE Transactions on Power Electronics*, 2015, 30(1): 471-481.

[10] LI S H, WANG X L, YAO Z Q, et al. Circulating current suppressing strategy for MMC-HVDC based on nonideal proportional resonant controllers under unbalanced grid conditions [J]. *IEEE Transactions on Power Electronics*, 2015, 30(1): 387-397.

[11] CHEN K, ZHANG Y W, ZHANG Z, et al. Proportion integration differentiation (PID) control strategy of belt sander based on fuzzy algorithm [J]. *Journal of Donghua University (English Edition)*, 2023, 40(2): 177-184.

[12] LIANG B Y, ZHENG S Q, AHN C K, et al. Adaptive fuzzy control for fractional-order

interconnected systems with unknown control directions [J]. *IEEE Transactions on Fuzzy Systems*, 2022, 30(1): 75-87.
[13] MA M, WANG T, QIU J B, et al. Adaptive fuzzy decentralized tracking control for large-scale interconnected nonlinear networked control systems [J]. *IEEE Transactions on Fuzzy Systems*, 2021, 29(10): 3186-3191.
[14] JAFARI M, MALEKJAMSHIDI Z, LU D D C, et al. Development of a fuzzy-logic-based energy management system for a multiport multioperation mode residential smart microgrid [J]. *IEEE Transactions on Power Electronics*, 2019, 34(4): 3283-3301.
[15] KARIMI A, KHAYAT Y, NADERI M, et al. Inertia response improvement in AC microgrids: a fuzzy-based virtual synchronous generator control [J]. *IEEE Transactions on Power Electronics*, 2020, 35(4): 4321-4331.
[16] ANDALIB-BIN-KARIM C, LIANG X D, ZHANG H G. Fuzzy-secondary-controller-based virtual synchronous generator control scheme for interfacing inverters of renewable distributed generation in microgrids [J]. *IEEE Transactions on Industry Applications*, 2018, 54(2): 1047-1061.
[17] NEVES R V A, MACHADO R Q, OLIVEIRA V A, et al. Multitask fuzzy secondary controller for AC microgrid operating in stand-alone and grid-tied mode [J]. *IEEE Transactions on Smart Grid*, 2019, 10(5): 5640-5649.
[18] HASANIEN H M, MATAR M. A fuzzy logic controller for autonomous operation of a voltage source converter-based distributed generation system [J]. *IEEE Transactions on Smart Grid*, 2015, 6(1): 158-165.
[19] ARCOS-AVILES D, PASCUAL J, MARROYO L, et al. Fuzzy logic-based energy management system design for residential grid-connected microgrids [J]. *IEEE Transactions on Smart Grid*, 2018, 9(2): 530-543.
[20] BAGHAEE H R, MIRSALIM M, GHAREHPETIAN G B. Performance improvement of multi-DER microgrid for small- and large-signal disturbances and nonlinear loads: novel complementary control loop and fuzzy controller in a hierarchical droop-based control scheme [J]. *IEEE Systems Journal*, 2018, 12(1): 444-451.
[21] VAFAMAND N, KHOOBAN M H, DRAGIČEVIĆ T, et al. Robust non-fragile fuzzy control of uncertain DC microgrids feeding constant power loads [J]. *IEEE Transactions on Power Electronics*, 2019, 34(11): 11300-11308.

基于模糊逻辑的微电网自适应下垂控制与环流抑制

王子平，单英浩*
东华大学 信息科学与技术学院，上海 201620

摘　要：微电网内部的环流会增加微电网的功率损耗，降低运行效率，以及影响微电网的电能质量。现有文献较少涉及利用模糊逻辑控制来抑制环流的方法。该文提出一种基于模糊控制下垂系数的方法来抑制微电网内部的环流，该方法将模糊控制与下垂控制相结合，通过自适应调整下垂系数，使每个子网之间的功率分配更加均衡，从而达到抑制环流的效果。为验证所提方法，在 Matlab/Simulink 环境下进行仿真，仿真结果表明所提方法明显优于传统的比例积分控制方法，环流从 10 A 左右降低到数纳安，母线电压和频率跌落情况也得到了明显改善，输出电压的总谐波失真率从 4.66%降低到 1.06%。此外，该文所用方法还可以拓展应用于多逆变器并联的情况，仿真结果表明该方法对抑制多个逆变器之间环流有良好的效果。

关键词：环流抑制；微电网；模糊逻辑；下垂控制